Tensor-Based Approaches to fMRI Classification

Vida John, Katherine Keegan, Tanvi Vishwanath, Yihua Xu; Advised by Elizabeth Newman

Emory University REU 2021: Computational Mathematics for Data Science

DMS-2051019

EMORY

Abstract

To analyze the abundance of multidimensional data, tensor-based frameworks have been developed. Traditional matrix-based frameworks extract the most relevant features of vectorized data using the matrix-SVD. However, we may lose crucial high-dimensional relationships in this process. To facilitate efficient multidimensional feature extraction, we propose a projection-based classification algorithm using the t-SVDM, a tensor-based extension of the matrix-SVD. We apply our algorithm to the StarPlus fMRI dataset.

Motivation - Matrix vs. Tensor

Matrix Method

- Uses matrix Singular Value Decomposition (SVD)
- Widely used in image processing
- Cannot identify relationships in higher dimensions

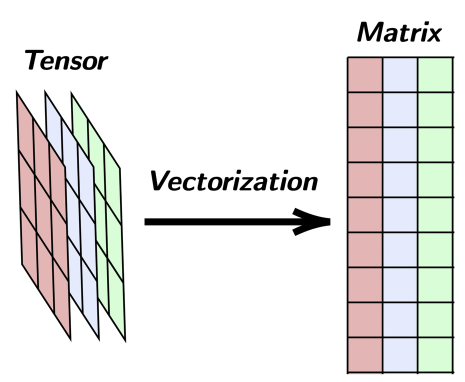

Figure 1:Turning multidimensional data into a matrix

Tensor Method

- Better representation of high-dimensional structure
- Flexibility in choosing a transformation $\boldsymbol{M}$

Background

- The **mode-k product** [5] refers to the multiplication of a matrix $\boldsymbol{M}$ along the k^{th} dimension of the tensor.
- **$\star_{\mathrm{M}}$-product:** [3] Given tensors $\boldsymbol{\mathcal{A}} \in \mathbb{R}^{n_1 \times n_2 \times n_3}$, $\boldsymbol{\mathcal{B}} \in \mathbb{R}^{n_2 \times \ell \times n_3}$, and an invertible $\boldsymbol{M} \in \mathbb{R}^{n_3 \times n_3}$:
$$\boldsymbol{\mathcal{C}} = \boldsymbol{\mathcal{A}} \star_{\mathrm{M}} \boldsymbol{\mathcal{B}} = (\hat{\boldsymbol{\mathcal{A}}} \triangle \hat{\boldsymbol{\mathcal{B}}}) \times_3 \boldsymbol{M}^{-1}$$
where $\boldsymbol{\mathcal{C}} \in \mathbb{R}^{n_1 \times \ell \times n_3}$.
- Figure 2 shows the t-SVDM of a tensor $\boldsymbol{\mathcal{A}}$.

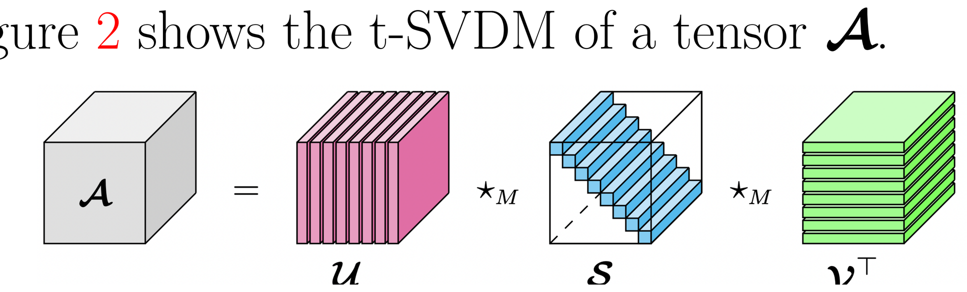

Figure 2:t-SVDM for third-order tensors [4]

Classification via Local t-SVDM

We extend the algorithm in [7] to higher-order tensors and the $\star_{\mathrm{M}}$-product.

Preprocessing

1. Split training data $\boldsymbol{\mathcal{A}}$ into c distinct classes:
$$\boldsymbol{\mathcal{A}}_1, \boldsymbol{\mathcal{A}}_2, \ldots, \boldsymbol{\mathcal{A}}_c$$
2. For each class i, compute t-SVDM and store first k basis elements:
$$\boldsymbol{\mathcal{A}}_i = \boldsymbol{\mathcal{U}}_i \star_{\mathrm{M}} \boldsymbol{\mathcal{S}}_i \star_{\mathrm{M}} \boldsymbol{\mathcal{V}}_i^\top \qquad \boldsymbol{\mathcal{U}}_{i,k} = \boldsymbol{\mathcal{U}}_i(:, 1:k, :)$$

Classifying a Test Image $\boldsymbol{\mathcal{T}}$

1. Project $\boldsymbol{\mathcal{T}}$ onto space spanned by each class basis:
$$\boldsymbol{\mathcal{P}}_i = \boldsymbol{\mathcal{U}}_{i,k} \star_{\mathrm{M}} \boldsymbol{\mathcal{U}}_{i,k}^\top \star_{\mathrm{M}} \boldsymbol{\mathcal{T}}, \text{ for } i = 1, \ldots, c$$
2. Categorize $\boldsymbol{\mathcal{T}}$ as the class whose projection was 'closest' to the original image:
$$i^* = \operatorname*{arg\,min}_{i=1,\ldots,c} \|\boldsymbol{\mathcal{T}} - \boldsymbol{\mathcal{P}}_i\|_F.$$

To measure the performance of our algorithm,
$$\text{accuracy} = \frac{\text{\# correctly classified images}}{\text{\# images}}$$

Intuition - MNIST [6]

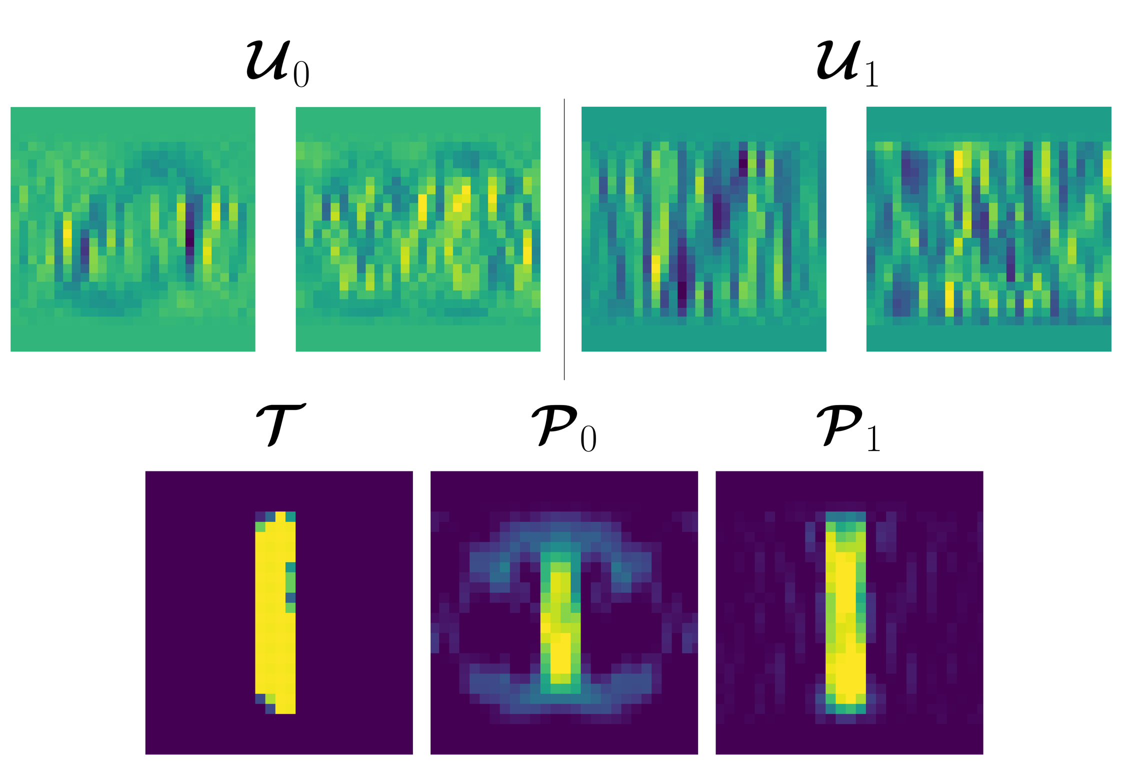

Figure 3:Illustration of classifying two digits of the MNIST Dataset using the local t-SVDM algorithm. Bases $\boldsymbol{\mathcal{U}}_0$ and $\boldsymbol{\mathcal{U}}_1$ are generated by digits from class 0 and class 1, respectively. We project $\boldsymbol{\mathcal{T}}$ onto the spaces spanned by $\boldsymbol{\mathcal{U}}_0$ and $\boldsymbol{\mathcal{U}}_1$ and obtain $\boldsymbol{\mathcal{P}}_0$ and $\boldsymbol{\mathcal{P}}_1$, respectively.

- $\boldsymbol{\mathcal{P}}_0$ has characteristics of both digit 0 and digit 1
- $\boldsymbol{\mathcal{P}}_1$ retains the characteristics of digit 1 only
- $\|\boldsymbol{\mathcal{T}} - \boldsymbol{\mathcal{P}}_0\|_F \approx 1.46 > \|\boldsymbol{\mathcal{T}} - \boldsymbol{\mathcal{P}}_1\|_F \approx 0.61$
- $\boldsymbol{\mathcal{T}}$ classified as a 1

StarPlus fMRI Data [2]

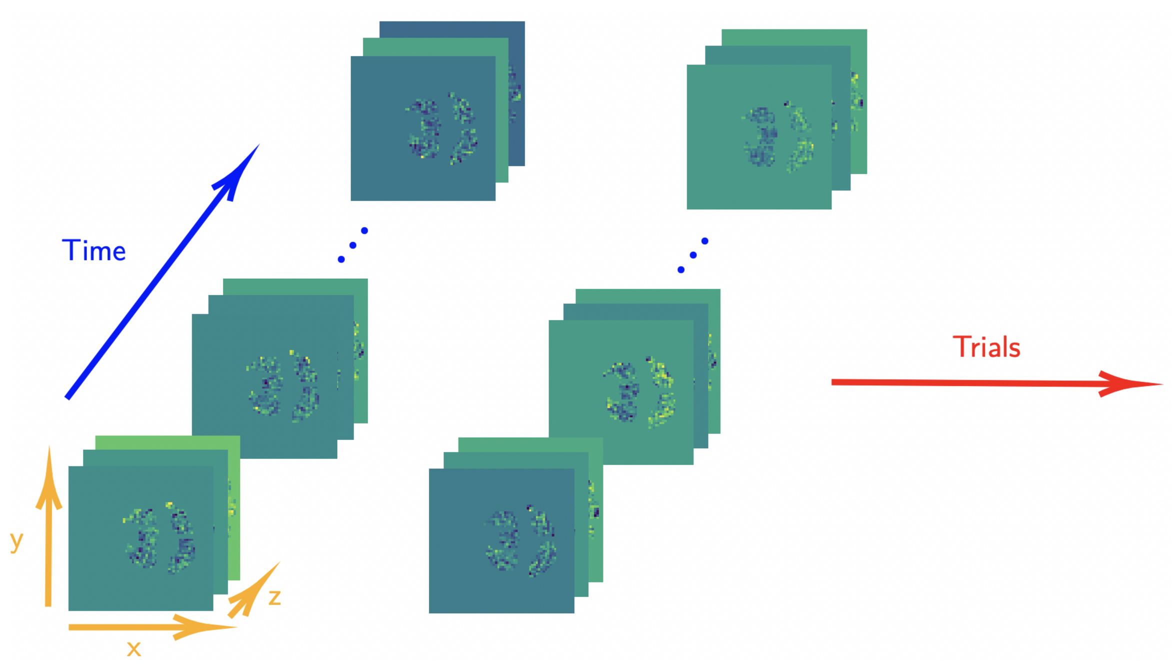

Figure 4:(trials, x, y, z, time) = (480, 64, 64, 8, 16)

The StarPlus fMRI data consists of six human subjects completing 80 trials, each corresponding to the distinct cognitive tasks of viewing either a picture or a sentence. The data is marked with anatomically-defined Regions of Interest (ROI's).

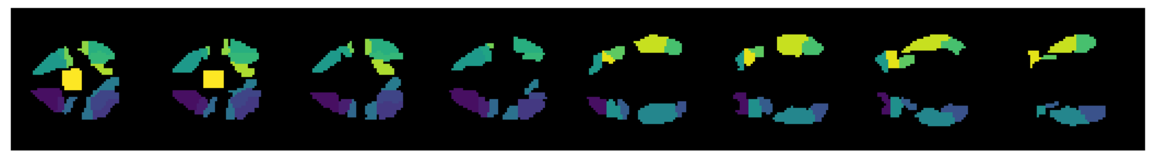

Figure 5:Twenty-five labeled Regions of Interest (ROIs)

Power of Tensor Representations

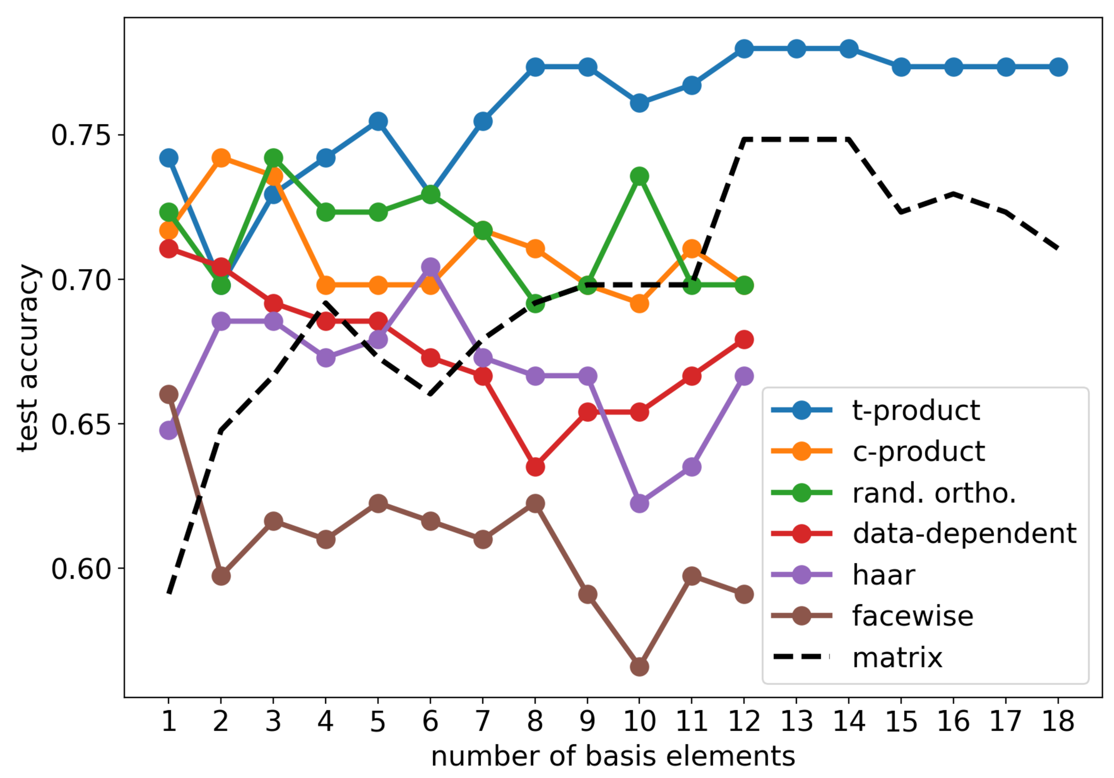

Figure 6:Test accuracy with respect to number of basis elements for various choices of $\star_{\mathrm{M}}$-product.

- Traditional matrix method overlooks the intrinsic characteristics of fMRI images as brain slices over time are very interconnected
- Tensor method outperforms matrix method in test accuracy with:
  - appropriate choice of transformation matrix $\boldsymbol{M}$
  - small number of basis elements

Impact of Brain Regions

We also experiment with an ROI-dependent $\boldsymbol{M}$ calculated from the most prominent ROI's in each trial.

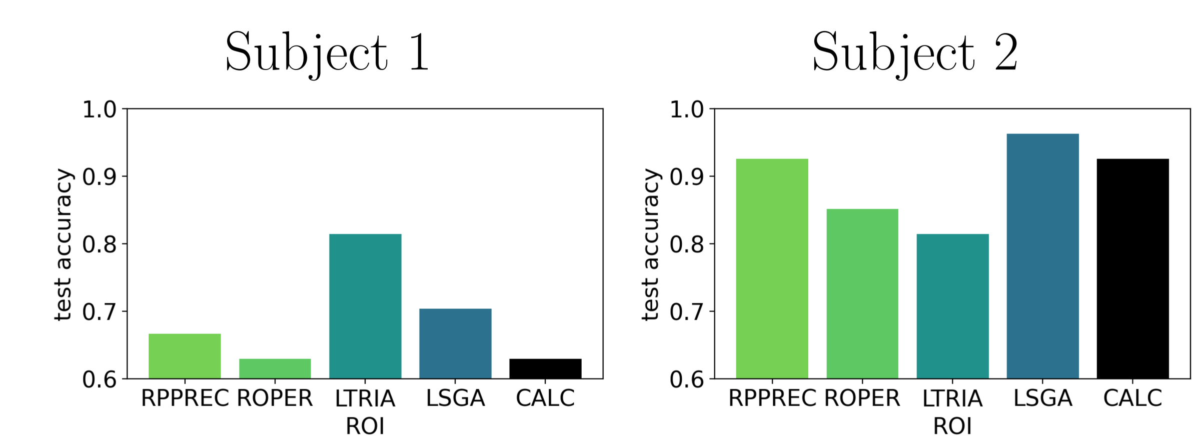

Figure 7:Results with ROI-dependent $\boldsymbol{M}$ for two subjects [a]

- Best ROI's vary depending on the subject
- No specific regions consistently improve performance in all subjects
- Illustrates how humans complete these cognitive tasks differently, demonstrating the difficulty of creating a good universal basis $\boldsymbol{\mathcal{U}}$

Conclusions and Future Work

- Local t-SVDM classification approach outperforms the equivalent matrix-based approach
- The most important brain regions for classification vary depending on the human subject
- Explore applications in disease prevention and diagnosis by utilizing other fMRI datasets
- Compare to other tensor-based frameworks such as Higher-Order SVD [5]

Reference

[1] Brain: Temporal lobe, vagal nerve, frontal lobe. https://my.clevelandclinic.org/health/diseases/16799-brain-temporal-lobe-vagal-nerve--frontal-lobe. Cleveland Clinic.

[2] M. Just. Starplus fmri data. Center for Cognitive Brain Imaging at Carnegie Mellon University.

[3] E. Kernfeld, M. Kilmer, and S. Aeron. Tensor–tensor products with invertible linear transforms. *Linear Algebra and its Applications*, 485:545–570, 11 2015.

[4] M. E. Kilmer, L. Horesh, H. Avron, and E. Newman. Tensor-tensor algebra for optimal representation and compression of multiway data. *Proceedings of the National Academy of Sciences*, 118(28), 2021.

[5] T. G. Kolda and B. W. Bader. Tensor decompositions and applications. *SIAM Review*, 51(3):455–500, September 2009.

[6] Y. LeCun and C. Cortes. MNIST handwritten digit database. 2010.

[7] E. Newman, M. Kilmer, and L. Horesh. Image classification using local tensor singular value decompositions. In *2017 IEEE 7th International Workshop on Computational Advances in Multi-Sensor Adaptive Processing (CAMSAP)*, pages 1–5, 2017.

[a] RPPREC = right posterior precentral sulcus, ROPER = right opercularis, LTRIA = left triangularis, LSGA = supramarginal gyrus, CALC = calcarine sulcus [1]